



# Fabrication of electrochemical sensor based on molecularly imprinted polymers for monitoring chlorpyrifos in real samples

DAMNITA SINGH<sup>1</sup>, NEELAM VERMA<sup>1,\*</sup>, RANJEETA BHARI<sup>2</sup> and KULDEEP KUMAR<sup>3</sup>

<sup>1</sup>Biosensor Laboratory Technology, Department of Biotechnology and Food Technology, Punjabi University, Patiala 147002, India

<sup>2</sup>Carbohydrate and Protein Biotechnology Laboratory, Department of Biotechnology and Food Technology, Punjabi University, Patiala 147002, India

<sup>3</sup>Department of Biotechnology, Mutani Mal Modi College, Patiala 147001, India

\*Author for correspondence (verma.neelam2@gmail.com)

MS received 4 May 2023; accepted 10 October 2023

**Abstract.** Chlorpyrifos (CPF) is an organophosphate pesticide that has been used for decades to enhance crop yield but its persistent usage has led to dreadful health issues in humans as well as other species. In the current work, an electrochemical sensor has been fabricated with immobilized molecularly imprinted polymers (MIPs) on a glassy carbon electrode to detect CPF. MIPs were bulk polymerized with a functional monomer itaconic acid. MIPs were characterized by Fourier transform infrared spectroscopy, scanning electron microscope, cyclic voltammetry and electrochemical impedance spectroscopy. The execution of the developed electrochemical sensor was scrutinized with differential pulse voltammetry (DPV). Various parameters like the pH of the electrolyte, the concentration and volume of MIPs (after elution), and the adsorption time were optimized for the analysis of the analyte (CPF) with the fabricated sensor. Under optimal conditions, the peak current of different CPF concentrations was examined by DPV method. The peak current was in linear proportionality with CPF ( $2.8 \times 10^{-14}$  to  $2.8 \times 10^{-5}$  mol l<sup>-1</sup>) with a low detection limit of  $1.912 \times 10^{-14}$  mol l<sup>-1</sup>. The developed electrochemical sensor detected CPF in real samples with excellent results and a recovery percentage ranging from 100 to 106% (relative standard deviation, RSD < 5%). Also, the sensor exhibited good reproducibility, stability and selectivity. Therefore, the developed electrochemical sensor holds great potential for the monitoring of CPF in fruits and vegetables.

**Keywords.** Chlorpyrifos; molecularly imprinted polymers; glassy carbon electrode; electrochemical sensor; itaconic acid; differential pulse voltammetry.

## 1. Introduction

A pesticide is a chemical/biological substance that protects the crop from damage caused by pests that can challenge humans for food and habitation while spreading diseases. Improper application of pesticides in agriculture and the health sector is not only deleterious to the environment, but also destroys non-target pest organisms (pollinators and predators), impairs biological diversity, and corrupts the soil microbial heterogeneity. According to their efficacy, and physical and chemical composition, the pesticides are categorized as organochlorines, organophosphates, carbamates, pyrethrin and pyrethroids [1]. Out of these pesticides stated above, organophosphates hold the utmost importance because of their comparatively higher efficacy. They work by damaging a crucial neurotransmitter, acetylcholinesterase (AChE), and cause twitching of voluntary muscles, which leads to paralysis and death of the pest, alongside, causing unwanted side effects in exposed humans.

Chlorpyrifos (CPF) is an organophosphate that has long been used to protect crops, vegetables and fruits from pests and to increase crop yield. It has been used extensively for agriculture, domestic and industrial purposes in recent years in India and its increasing use contributes to potential health risks. CPF residues in vegetables, fruits and water are harmful to humans as well as animals because they lead to fatal diseases, and are toxic to aquatic organisms and honeybees [2]. Lately, it appears that the number of poisoning cases and deaths has grown manifold, still, it is not banned, so its detection has become the primary concern as it can pave the way for suitable remediation of CPF intoxication in the environment

CPF has adverse effects on many non-target organisms like birds, bees, fishes and even humans. For instance, certain bird species like Mallard ducks when coming in contact with CPF, lay fewer eggs and not many ducklings survive because it leads to the thinning of egg shells. It accumulates in the tissues of aquatic invertebrates and

fishes and proves to be highly toxic. Its toxicity towards honey bees has gained a lot of attention. They suffer from memory deficits even with a small dosage of CPF [3]. CPF enters the human body through inhalation, oral exposure or by direct contact [4]. It is absorbed in the blood and the symptoms emerge within 2 h of ingestion. Reversible peripheral neuropathies and polyneuritis have been observed in humans owing to acute exposures, whereas dermal exposure results in skin flushing. Other symptoms include reduced tendon reflexes, weakness in the muscles of the face, neck and proximal limb, cranial nerve palsies, along with partial respiratory paralysis [5].

The monitoring of CPF residue in food items, water and soil is very crucial to ensure that their concentration in the ecological system is below the permissible levels. Many analytical methods such as mass spectrometry, enzyme-linked immunosorbent assay, gas chromatography, liquid chromatography and high-performance liquid chromatography (HPLC) have been employed for CPF detection. Although these methods are sensitive, selective and reproducible, they are time intensive, laborious and expensive [6]. Molecularly imprinted polymer technology overcomes all the limitations of analytical methods and provides a convenient technique for CPF detection.

Molecular imprinting technology (MIT) is defined as a technique of fabricating the molecular lock for a molecular key [7], where a functional group and a crosslinker are polymerized in the presence of a template, followed by the removal of the template from the polymer network to leave a template-fitted cavity [8]. Over the past few decades, MIT has become an emerging technique for creating binding sites on the polymer matrix [9,10]. Recently, the focus on MIPs in sensor development has sharpened because of their high affinity, selectivity, stability and low fabrication cost [1,11].

MIPs are potentially used in the detection of various compounds in food even those which are found in low concentrations. They are implemented for the identification of volatile organic compounds (like vanillin, D-limonene) and off-odour compounds (like herbs and wines) found in food [12]. MIPs have been widely employed for detecting contaminants like pesticides (like methyl parathion, triazophos, carbofuran, phoxim), veterinary drugs (like estradiol, cloxacillin, salbutamol), packaged food contaminants (like bisphenol A, patuline, diisononyl phthalate), natural toxins (like tyramine, histamine), bacterial contaminants (*N*-acyl-homoserine-lactones) and mycotoxins (like citrinin, zearalenone) [13].

Lately, the direct synthesis of MIPs with electro-polymerizable monomers on the surface of the electrode by the process of electropolymerization (EP) has gained traction owing to their affordability and convenience of use. Electrochemical sensors (ECS) convert an analyte's interaction with a receptor on the surface of an electrode into an analytical signal. Voltammetry, amperometry, potentiometry, conductivity and capacitance or impedance changes are

among the electroanalytical techniques used by these sensors. MIP-ECS have fulfilled the need for satisfactory sensing efficacy for environmental applications by demonstrating incredibly better low detection limit ranges.

In the present study, MIPs were synthesized for the detection of CPF (template) using itaconic acid as a functional monomer. The characterization of synthesized MIPs was accomplished by scanning electron microscope and Fourier transform infrared spectroscopy (FTIR). The electrochemical behaviour of the developed sensor was illustrated by cyclic voltammetry (CV) and electrochemical impedance spectroscopy (EIS). When compared with other ECS, it exhibited a wide range and low LOD (limit of detection). The applicability of the fabricated sensor was evaluated by quantifying CPF in real samples like apples, cucumber, water and pomegranate.

## 2. Experimental

Chlorpyrifos (CPF), ethylene glycol dimethacrylate (EGDMA), and itaconic acid were procured from Sigma-Aldrich; azobisisobutyronitrile (AIBN) from Loba Chemie Private Limited; potassium ferricyanide ( $K_3[Fe(CN)_6]$ ), acetonitrile and potassium ferrocyanide ( $K_4[Fe(CN)_6] \cdot 3H_2O$ ) from S-D Fine Chemicals Limited; methanol and potassium chloride (KCl) from HIMEDIA and acetic acid and dimethylformamide (DMF) from Merck Specialities Private Limited. In the entire experimentation, Milli-Q deionized (DI) water analytical grade chemicals were employed.

Electrochemical analysis was conducted at room temperature using a CHI660C electrochemical workstation. The three-electrode system was implemented, where glassy carbon electrode (GCE; 3 mm diameter), Ag/AgCl and platinum wire were employed as working, reference and auxiliary electrodes, respectively.

## 3. Synthesis of MIPs and non-imprinted polymers

MIPs were synthesized by bulk polymerization method as described by Hasanah *et al* [14] with modifications like a different template, functional monomer, and molar ratio. CPF was used as the template, itaconic acid as the monomer, AIBN as the initiator, EGDMA as the cross-linker, and acetonitrile as the porogen. Template, monomer, and cross-linker were employed in the molar ratio of 1:4:25 for MIPs synthesis. Pre-polymerization solution contained CPF, itaconic acid, and EGDMA in acetonitrile (10 ml). It was sonicated at RT (room temperature) for 15 min at 60% amplitude before the addition of AIBN followed by nitrogen purging for 5 min. The solution was capped and placed in the water bath for 1 hour at 80°C. The temperature of the water bath was reduced to 60°C and the solution was retained for 24 h. The polymers obtained were washed with

methanol, dried, and crushed for further experiments. Non-imprinted polymers (NIPs) were synthesized simultaneously under similar conditions without the template.

### 3.1 Template extraction

CPF was extracted by washing the polymers with methanol and acetic acid (9:1, v/v). 10 mg MIPs were added to 1 ml methanol: acetic acid (9:1, v/v). It was sonicated for 5 min at room temperature at 70% amplitude and kept in a shaking incubator set at 150 rpm at room temperature. The solution was collected every 2 h and monitored via UV-Vis spectrophotometer till the template was completely removed.

## 4. Preparation of electrochemical sensor

### 4.1 Pretreatment of GCE

GCE was mechanically polished using 0.3  $\mu\text{m}$ , 0.1  $\mu\text{m}$  and 0.05  $\mu\text{m}$  alumina powder on a soft polishing cloth. The electrodes were rinsed with deionized water and dried under nitrogen gas.

### 4.2 Fabrication of molecularly imprinted electrochemical sensor

MIPs after elution were dispersed in 5 ml DMF (different concentrations were taken into account for the study, 0.5 to 5  $\text{mg ml}^{-1}$ ). An aliquot of 5  $\mu\text{l}$  of eluted MIPs dispersion was dropped on pre-treated GCE and air-dried. Eluted MIPs and NIPs were also deposited on the electrode with the same procedure. Figure 1 illustrates the fabrication process of MIPs synthesis and CPF-imprinted electrochemical sensor.

## 5. Characterization

The structural morphology was acquired by scanning electron microscope (JOEL, JSM6010LV). Fourier transform infrared spectroscopy was performed for the identification of the compounds. Absorption spectra were operated on a fibre optic spectrophotometer (Maya2000, Oceanic Optics, USA).

Electrochemical characterization of MIPs and NIPs was determined by CV and EIS. CV measured the current response of MIPs, NIPs and MIPs after elution. The supporting electrolyte for CV was 5 mM potassium ferro-ferricyanide, the potential range was  $-0.6$  to  $0.6$  V and the scan rate was  $0.05$   $\text{V s}^{-1}$ . EIS was used to evaluate the impedance spectrum of the modified electrodes. The electrochemical solution for EIS was 5 mM potassium ferro-ferricyanide and 0.1 M potassium chloride.

## 6. Results

### 6.1 Characterization

The morphology of MIPs, NIPs and MIPs after elution was almost the same. The only difference observed was in the regularity of shape. As shown in figure 2, MIPs (a) have a regular shape as compared to NIPs (b) and MIPs after elution (c). This regular shape of MIPs could be due to the formation of polymers. After the extraction of the template, the shape of MIPs gets disrupted and becomes rough.

MIPs formation and CPF extraction were confirmed by FTIR spectra of MIPs, NIPs, eluted MIPs (template removed) and CPF. Figure 3 depicts the FTIR spectra (b) and band assignments (a) of CPF (I), MIPs (II), MIPs after elution (III) and NIPs (IV). The FTIR spectra of MIPs before template elution showed peaks around 2900 and at  $754.17$   $\text{cm}^{-1}$  corresponding to N-H and C-Cl stretching, respectively. After the extraction of the template, N-H and C-Cl stretch disappeared, confirming the extraction of CPF from the polymers. The stretching vibration of C=C around 1640 and  $1725$   $\text{cm}^{-1}$  in MIPs, NIPs and MIPs after elution indicates the polymerization of itaconic acid and EGDMA, thereby confirming the formation of polymers. The peak strength at  $1387.5$   $\text{cm}^{-1}$  in MIPs was higher than NIPs, which indicates the increase in -OH active groups and confirms the formation of binding sites for the template.

The current response of polymers was estimated by CV (figure 4). MIPs after elution (c) exhibit higher current response than MIPs before elution (a). This is due to the appearance of imprinted cavities in MIPs after CPF elution, which promotes the passage of electrochemical solution thus participating in a redox reaction. Before elution, the cavities were occupied by CPF, hindering the passage of electrolytes.

EIS was performed to study the resistance at each modification step of electrodes. Figure 5 demonstrates the impedance of MIPs (a), NIPs (b), MIPs after elution (c) and bare (d) electrodes. The impedance value of MIPs after elution tapered as compared to MIPs before elution because the cavities formed in eluted MIPs with the extraction of the template enhanced the electron transfer process.

### 6.2 Optimization of experimental conditions

**6.2a pH of the electrolyte:** The pH of the electrolyte (potassium ferro-ferricyanide and phosphate buffer saline) is the important parameter for the electrochemical detection of the template. The differential pulse voltammetry (DPV) response was investigated with the selected electrolyte at a pH range of 5–10 (figure 6a). The best peak current was found at pH 7.

**6.2b Eluted MIPs concentration:** The effect of MIPs (after elution) concentration (0.5 to 5  $\text{mg ml}^{-1}$ ) was estimated by

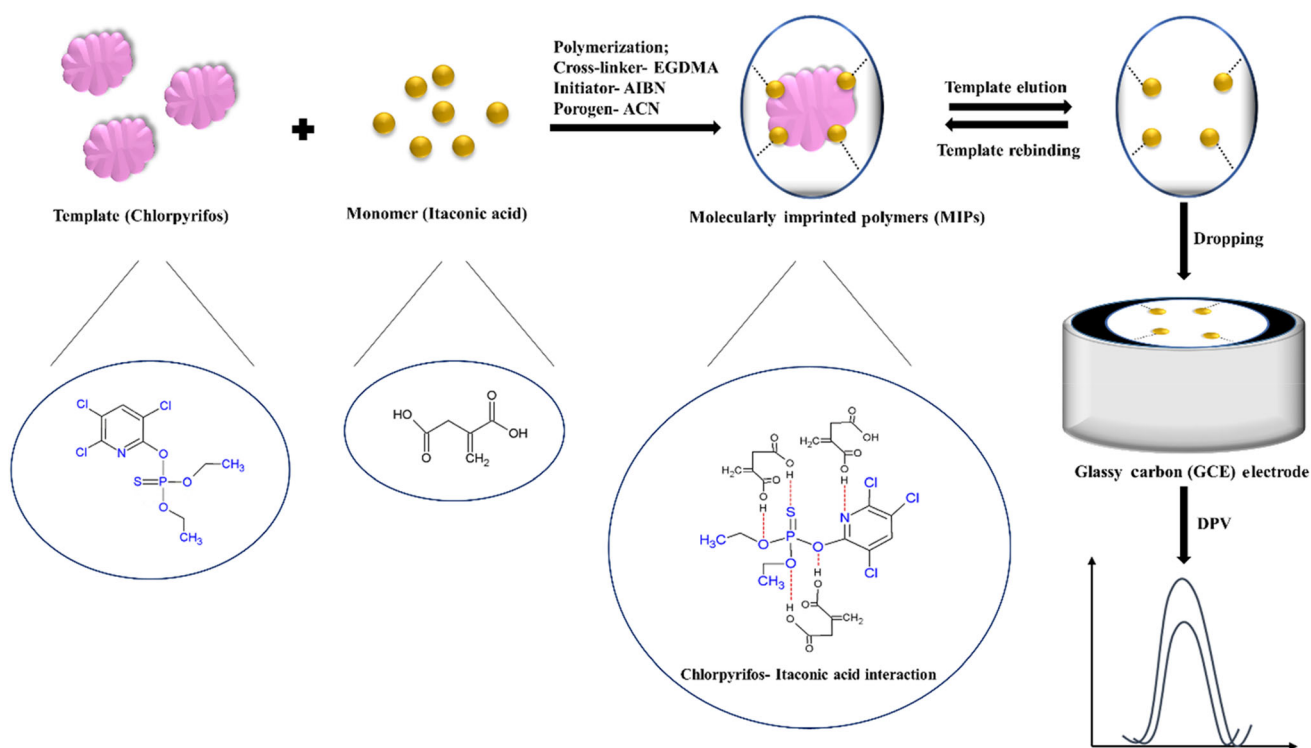


**Figure 1.** Fabrication process of MIPs synthesis and CPF imprinted electrochemical sensor.

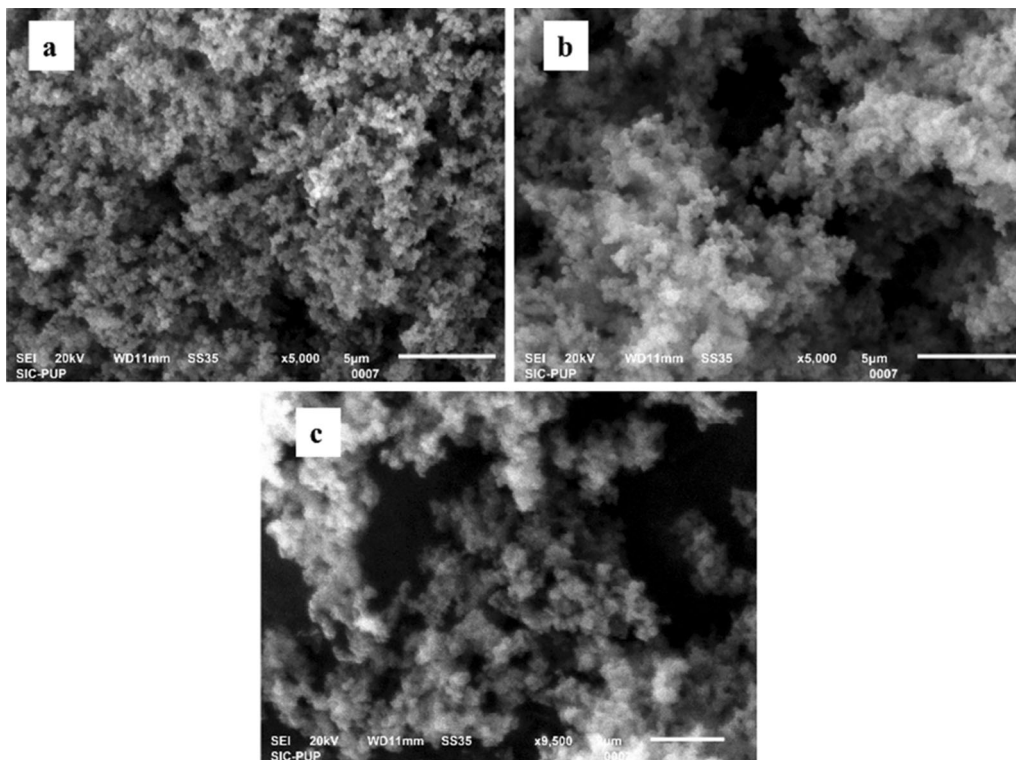


**Figure 2.** Scanning electron microscope images of (a) MIPs, (b) NIPs and (c) MIPs after elution

DPV at constant CPF concentration ( $2.85 \times 10^{-6} \text{ mol l}^{-1}$ ). With an increase in eluted MIPs concentration, the peak current ( $\Delta I$ ) increases from  $0.5 \text{ mg ml}^{-1}$  to  $3.5 \text{ mg ml}^{-1}$  but a further increase embarks the decrease in peak value as

illustrated in figure 6b. This decrease can be attributed to the increase in absorption of CPF, which leads to reduced current response. A concentration of  $3.5 \text{ mg ml}^{-1}$  of eluted MIPs was selected for further studies.

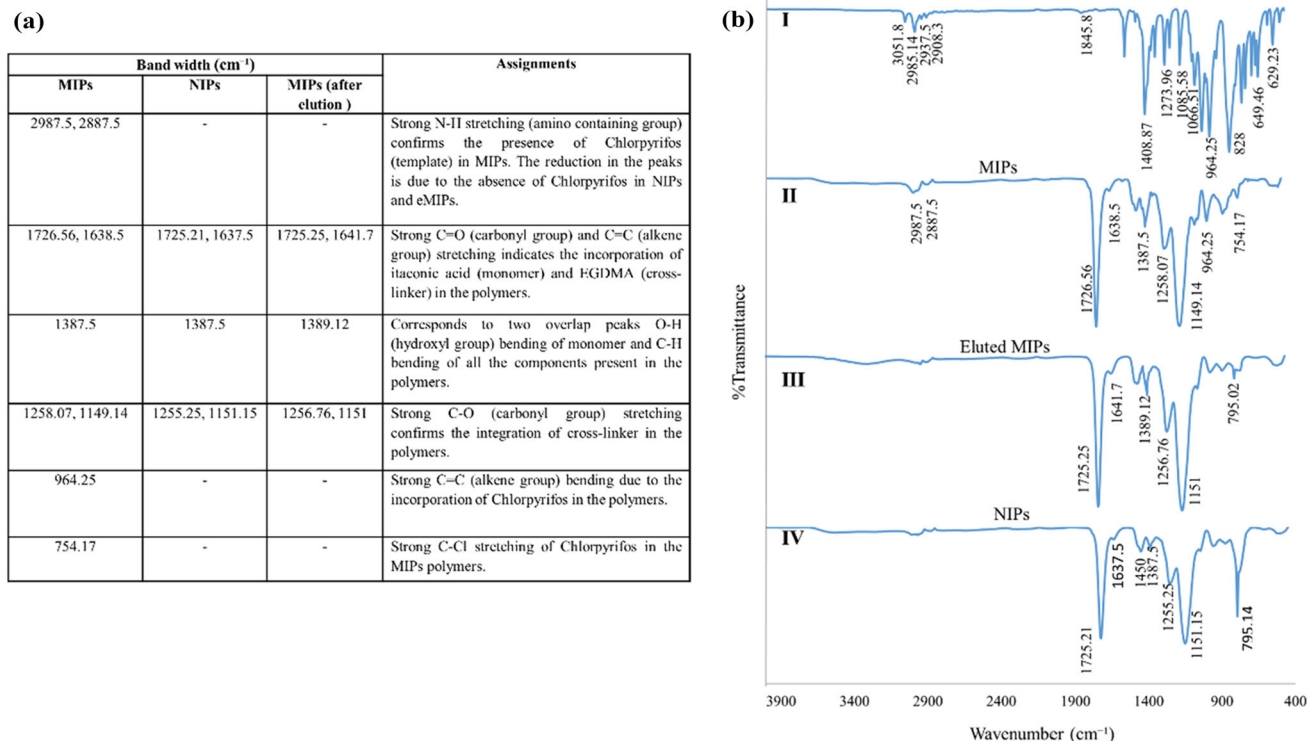


**Figure 3.** (a) Band assignments of MIPs, NIPs, MIPs after elution and (b) FTIR spectra of CPF (I), MIPs (II), MIPs after elution (III) and NIPs (IV).

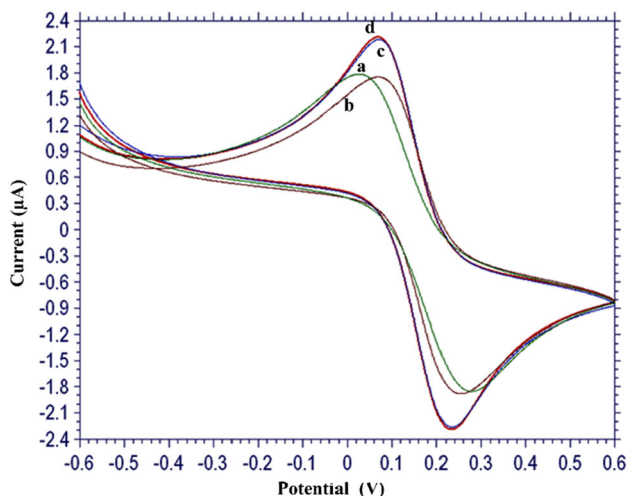


**Figure 4.** Cyclic voltammograms of (a) MIPs, (b) NIPs, (c) MIPs after elution and (d) bare were recorded in 5 mM potassium ferro/ferri cyanide.

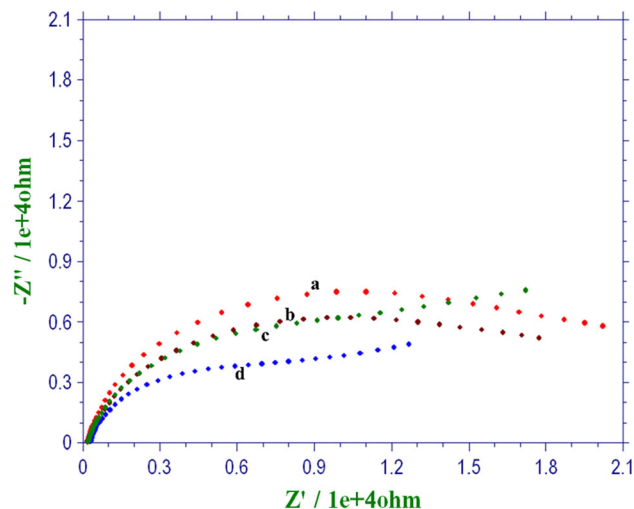


**Figure 5.** The EIS of (a) MIPs, (b) NIPs, (c) MIPs after elution and (d) bare were recorded in 5 mM potassium ferro/ferri cyanide and 0.1 M potassium chloride.

**6.2c Volume of eluted MIPs:** The different volumes (5–25 µl) of eluted MIPs of selected concentration were dropped on the electrode and the respective DPV was recorded. Eluted MIPs of 15 µl illustrated the best peak current. Initially, the change in peak current ( $\Delta I$ ) bumps with the increase in the number of MIPs (after elution) but later on it drops (figure 6c).

**6.2d Adsorption time:** The adsorption time is a very important parameter for designing the sensor.  $2.85 \times 10^{-6}$  mol l<sup>-1</sup> concentration of CPF was selected for the studies. The change in the peak current was monitored for 600 s with intervals of 60 s. As portrayed in figure 6d, the peak current increased sharply till 240 s and reached saturation thereafter.

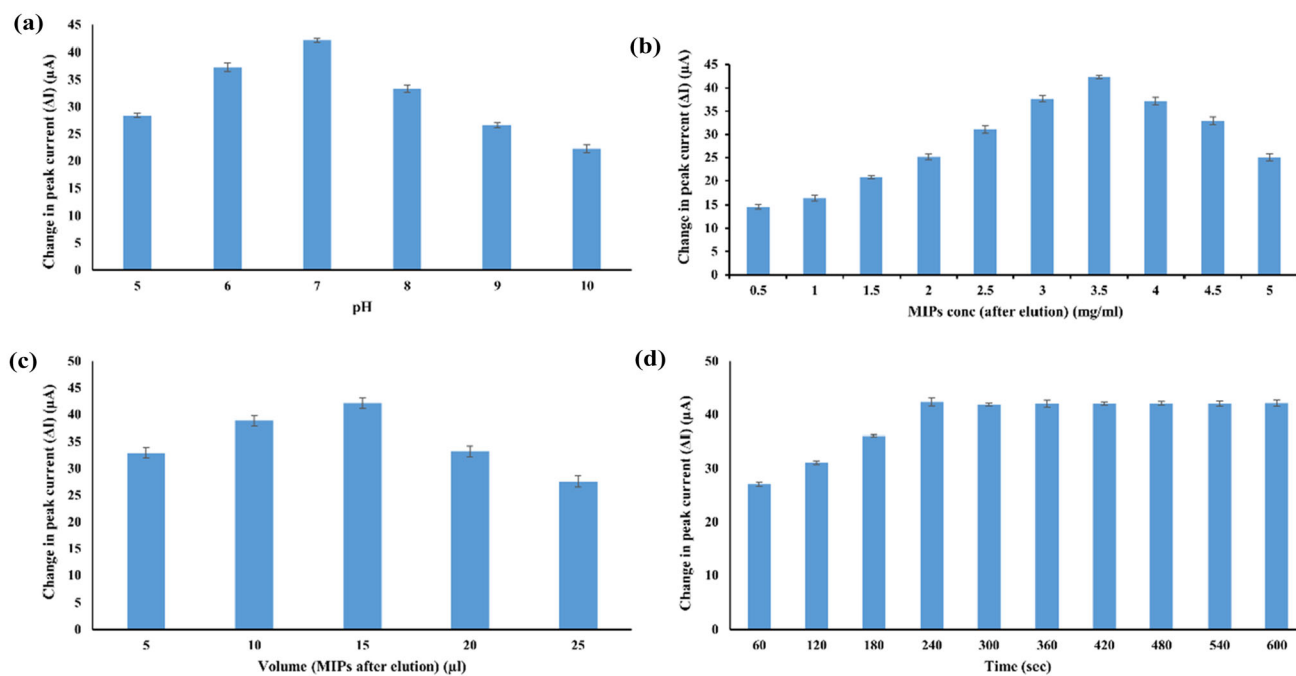


**Figure 6.** Experimental conditions optimized for the development of electrochemical sensor (a) pH of the electrolyte, (b) selection of concentration of MIPs, (c) amount of the selected MIPs concentration and (d) selection of absorption time.

### 6.3 Detection of CPF

The peak current of different CPF concentrations was recorded by DPV under the optimized conditions. The increase in the peak current from 22.52 to 61.93 μA was observed with the decrease in CPF concentration from  $2.8 \times 10^{-5}$  to  $2.8 \times 10^{-14}$  M (figure 7), this is due to more binding of the template at the polymer sites which limits the

electron transfer. CPF binds in the cavities/voids of polymers via hydrogen bonding between N, S and O groups of CPF and OH group of itaconic acid. During rebinding, increase in CPF level prompts the instant filling of voids that limits the dispersal of redox probe (ferrocyanide) ions, which results in poor redox kinetics, hence low current. Concurrently, the availability of redox probe ions escalates towards the surface of electrode at low concentrations of

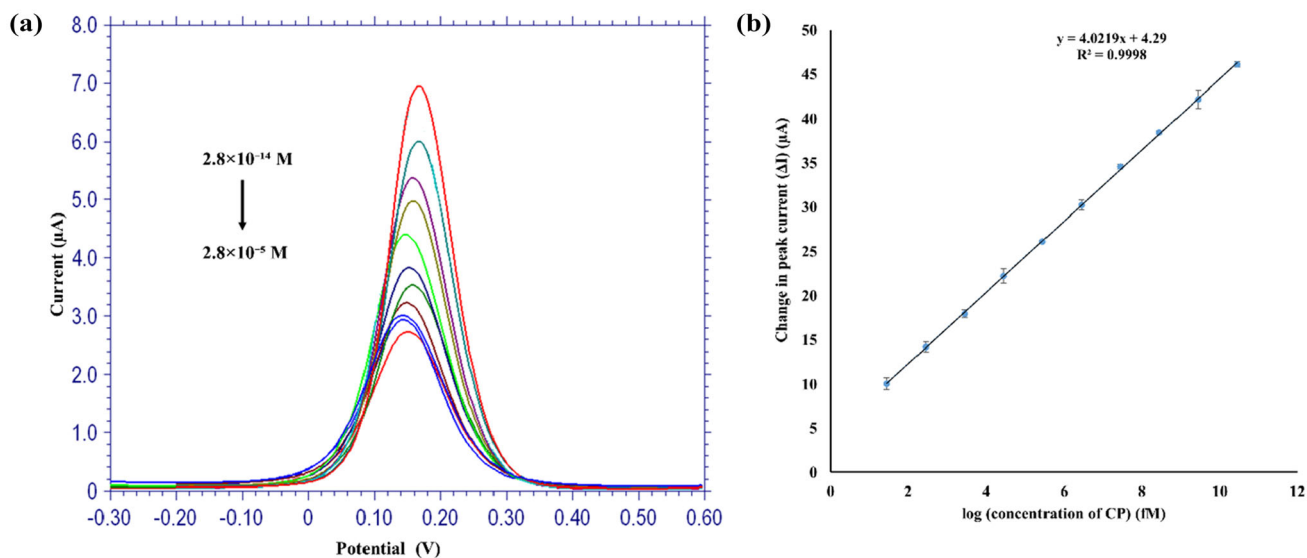


**Figure 7.** (a) DPV of various chlorpyrifos (CPF) concentration in the range from  $2.8 \times 10^{-5}$  to  $2.8 \times 10^{-14}$  M in 5 mM potassium ferro-ferricyanide and 0.1 M phosphate buffer saline, topmost peak is of MIPs (after elution). (b) The calibration curve of CPF detection.

**Table 1.** Comparison between present study and similar reported literature.

Monomer	MIPs	LOD (M)	Linear range (M)	References
Methacrylic acid	MIPs	$1.0 \times 10^{-13}$	$1.0 \times 10^{-12}$ to $2.0 \times 10^{-8}$	[15]
Methacrylic acid	MIPs coated on GCE	$4.08 \times 10^{-9}$	$1 \times 10^{-10}$ to $1 \times 10^{-5}$	[16]
Polypyrrole	Iridium oxide NPs embedded MIPs	$1 \times 10^{-13}$	$1 \times 10^{-13}$ to $1 \times 10^{-3}$	[17]
Methacrylic acid	MIPs and MWCNTs	$8.1 \times 10^{-13}$	$5 \times 10^{-12}$ to $5 \times 10^{-8}$	[18]
Itaconic acid	MIPs coated on GCE	$1.912 \times 10^{-14}$	$2.8 \times 10^{-14}$ to $2.8 \times 10^{-5}$	Present study

CPF, as less sites are occupied so more dispersal of redox probes which leads to higher current response. With the regression equation,  $y = 4.0159x + 4.026$  and  $R^2 = 0.9972$ , LOD was calculated and found to be  $1.912 \times 10^{-14}$  M (19.12 fM). Table 1 illustrates the comparison between the present work and already similar reported literature in the detection of CPF using MIPs-based sensors.

#### 6.4 Reproducibility

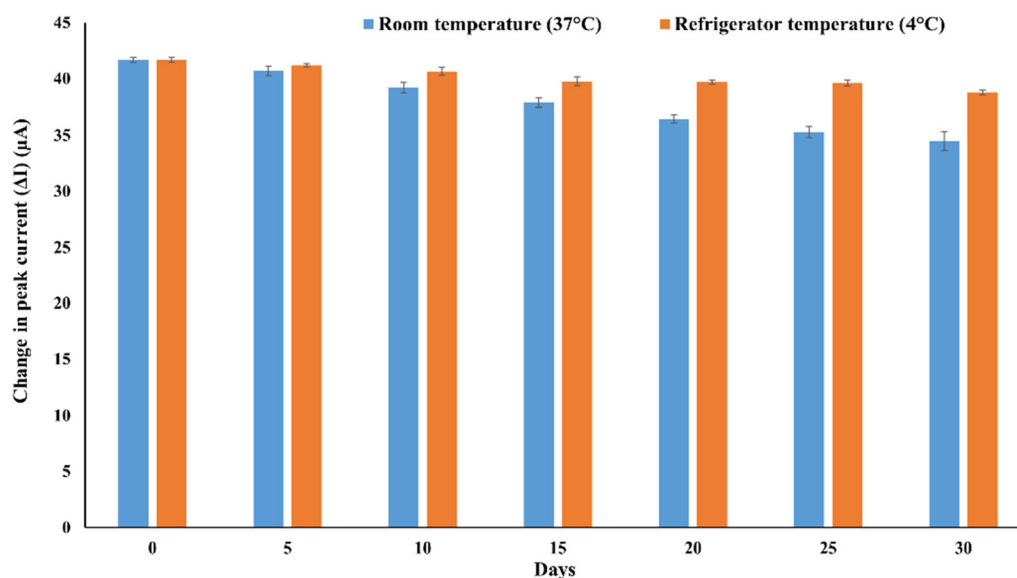
The reproducibility was investigated with the DPV response of the developed electrochemical sensor at  $2.85 \times 10^{-6}$  mol l<sup>-1</sup> CPF concentration with five identical electrodes prepared under similar conditions. The RSD was found to be 1.59% (table 2).

**Table 2.** Reproducibility of chlorpyrifos-imprinted electrochemical sensor.

MIPs sensors	Change in peak current ( $\Delta I$ ) ( $\mu$ A)	RSD (%)
1	42.29	1.59
2	42.08	
3	41.34	
4	41.42	
5	41.95	

#### 6.5 Stability

The stability of the developed sensor was determined by analysing the current response of  $2.85 \times 10^{-6}$  mol l<sup>-1</sup> CPF concentration at regular intervals of 5 days for 1 month stored at room (37°C) and refrigerator (4°C) temperature (figure 8). The RSD values at room and refrigerator temperatures were 1.216% and 0.626%, respectively, as shown in table 3. The sensor retained 82.84% and 92.97% of the response after 1 month at room and refrigerator temperatures, respectively. The results indicated that the refrigerated sensor was more stable as compared to room temperature.

**Figure 8.** Stability of chlorpyrifos-imprinted electrochemical sensor stored at room temperature and refrigerator temperature.

**Table 3.** Stability of chlorpyrifos-imprinted electrochemical sensor stored at room temperature and refrigerator temperature.

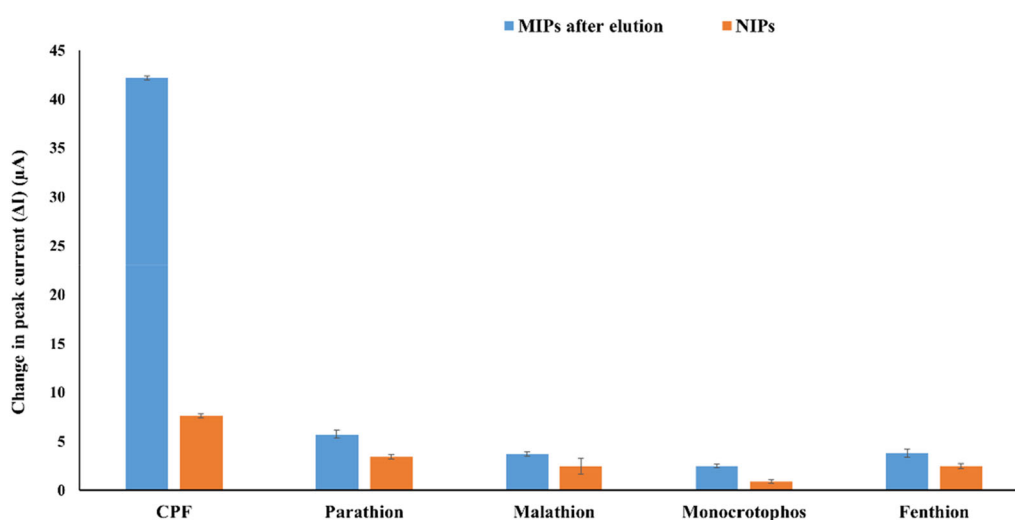
Days	Room temperature (37°C)	Refrigerator temperature (4°C)
0	41.645	41.645
5	40.673	41.171
10	39.165	40.638
15	37.877	39.751
20	36.46	39.689
25	35.305	39.58
30	34.501	38.719
RSD	1.216	0.626

### 6.6 Selectivity

The specificity was studied by investigating the current response of the electrode with other pesticides—parathion, malathion, monocrotophos and fenthion ( $2.8 \times 10^{-6}$  M). In figure 9, the current response of CPF is higher than the other pesticides. This confirms the specificity of the electrode for CPF.

### 6.7 Real sample analysis

The applicability of the developed sensor was evaluated by quantifying the CPF in real samples. Apple, cucumber and pomegranate were collected from a local market, and a

**Figure 9.** Specificity of the developed sensor with other pesticides at  $2.8 \times 10^{-5}$  M concentration.**Table 4.** Recoveries of chlorpyrifos from real samples.

Sample	Amount of CPF added (M)	Amount of CPF found (M)	Recovery (%)	RSD (%)
Apple	Unspiked	$3.23 \times 10^{-13}$	—	1.48
	$2.80 \times 10^{-12}$	$2.97 \times 10^{-12}$	106.04	1.69
	$2.80 \times 10^{-11}$	$2.82 \times 10^{-11}$	100.80	2.53
	$2.80 \times 10^{-10}$	$2.804 \times 10^{-10}$	100.17	5.08
Cucumber	Unspiked	$1.7 \times 10^{-13}$	—	1.87
	$2.80 \times 10^{-12}$	$2.95 \times 10^{-12}$	105.21	3.46
	$2.80 \times 10^{-11}$	$2.77 \times 10^{-11}$	98.97	1.18
	$2.80 \times 10^{-10}$	$2.80 \times 10^{-10}$	100.09	2.11
Pomegranate	Unspiked	$1.89 \times 10^{-14}$	—	2.28
	$2.80 \times 10^{-12}$	$2.81 \times 10^{-12}$	100.5	2.61
	$2.80 \times 10^{-11}$	$2.8 \times 10^{-11}$	100.11	2.19
	$2.80 \times 10^{-10}$	$2.8 \times 10^{-10}$	100.004	2.24
Water	Unspiked	$2.3 \times 10^{-13}$	—	3.79
	$2.80 \times 10^{-12}$	$2.74 \times 10^{-12}$	97.93	3.14
	$2.80 \times 10^{-11}$	$2.71 \times 10^{-11}$	96.76	1.52
	$2.80 \times 10^{-10}$	$2.75 \times 10^{-10}$	98.37	2.5



water sample was collected from the factory. CPF was extracted from the solid samples by crushing them using mortar and pestle and then immersing 10 mg of the sample in 10 ml acetonitrile and finally filtering via cellulose filter membrane (0.22  $\mu\text{m}$ ). Water samples were also refined via the cellulose filter membrane (0.22  $\mu\text{m}$ ) before use. These samples were then spiked with the known concentration of CPF ( $2.85 \times 10^{-10}$  M,  $2.85 \times 10^{-11}$  M,  $2.85 \times 10^{-12}$  M). Table 4 depicts the recoveries of CPF from real samples. The results indicate that the developed electrochemical sensor detects CPF in complex samples.

## 7. Discussion and conclusion

This study anthologizes the fabrication of an electrochemical sensor hinged on MIPs for the detection of CPF. On account of distinct framework and competent recognition, MIPs are extensively utilized in a variety of fields, particularly in molecularly imprinted electrochemical sensors (MIECS). ECS based on MIPs has substantially enhanced sensing performance in recent years by increasing surface area, conductivity and electrocatalytic activity, facilitating electron transport phenomena while offering a specific recognition effect. Furthermore, MIECS have a prudent construct, featuring a 3D porous surface framework, a core-shell structure, and a molecularly imprinted surface, that ought to decrease mass transfer resistance and in turn, improve sensitivity. New MIPs are developed in an effective way to improve selectivity by using dual functional monomers and integrating specific groups that can strongly bond with the template and form a particular donor–receptor conjugation.

In the present study, MIPs were bulk polymerized with Itaconic acid (IA) as a functional monomer. IA was selected for the synthesis on the assumption that it can form a hydrogen bond with the template (CPF). The synthesized MIPs were drop cast on GCE and the experimental conditions for the detection of CPF were optimized. Under optimum analytical conditions, the linear range and limit of detection were found to be ranging from  $2.8 \times 10^{-14}$  to  $2.8 \times 10^{-5}$  M and  $1.912 \times 10^{-14}$  M (19.12 fM), respectively. The sensor retained 92.97% of its response after refrigeration for 30 days. The applicability of the fabricated sensor was evaluated by quantifying the CPF in the complex real samples. The percentage recovery was found to be 100 to 106%, hence, the fabricated electrochemical sensor was proficient in detecting CPF in complex samples.

Although the continuous expansion of MIECS in the analysis is speculated at an impressive pace, there are still significant developmental challenges for commercial applications. These challenges must be addressed meticulously to exploit their applications in various fields. So far,

these molecularly imprinted ECS have limitations due to their functional complexity, limited solubility, low chemical and mechanical stability, reliance on less environmentally friendly reagents, and limited reusability. Scaling up the production process and attempting to improve the synthesized material while incorporating chemometric methods are some of the constraints. Overcoming these will result in lower-cost systems with greater reliability and efficiency in challenging circumstances, favouring the acquisition of a compatible receptor for any desired analytical agent.

## References

- [1] Abubakar Y, Tijjani H, Egbuna C, Adetunji C O, Kala S, Kryeziu T L *et al* 2019 *Nat. Remedies Pest Dis. Weed Control* p 29
- [2] Kumar N, Narayanan N and Gupta S 2019 *React. Funct. Polym.* **135** 103
- [3] Kushwaha A, Singh G and Sharma M 2020 *RCS Adv.* **10** 13050
- [4] Eaton D L, Daroff R B, Autrup H, Bridges J, Costa L G, Coyle J *et al* 2008 *Crit. Rev. Toxicol.* **38** 1
- [5] Rathod A L and Garg R K 2017 *J. Forensic Leg. Med.* **47** 29
- [6] Altaf R, Ullah Z, Darko D A, Iqbal A, Khan M S and Asif M 2022 *Asean J. Sci. Eng.* **2** 257
- [7] Chen L, Wang X, Lu W, Wu X and Li J 2016 *Chem. Soc. Rev.* **45** 2137
- [8] Hasanah A N, Safitri N, Zulfa A, Neli N and Rahayu D 2021 *Molecules* **26** 5612
- [9] Chen L, Xu S and Li J 2011 *Chem. Soc. Rev.* **40** 2922
- [10] Golker K, Karlsson B C G, Olsson G D, Rosengren A M and Nicholls I A 2013 *Macromolecules* **46** 1408
- [11] Mohammadi V, Saraji M and Jafari M T 2019 *Microchim. Acta* **186** 524
- [12] Cengiz N, Guclu G, Kelebek H, Capanoglu E and Selli S 2021 *ACS Omega* **7** 15258
- [13] Elfadil D, Lamaoui A, Della Pelle F, Amine A and Compagnone D 2021 *Molecules* **26** 1
- [14] Hasanah A N, Dwi Utari T N and Pratiwi R 2019 *J. Anal. Methods Chem.* **2019** 9853620
- [15] Lin G F, Wang Y H, Li G C, Bai W, Zhang H and Wang S C 2014 *Adv. Mater. Res.* **936** 843
- [16] Xu W, Wang Q, Huang W and Yang W 2017 *J. Sep. Sci.* **40** 4839
- [17] Capoferri D, Álvarez-Diduk R, Del Carlo M, Compagnone D and Merkoçi A 2018 *Anal. Chem.* **90** 5850
- [18] Huang W, Zhou X, Luan Y, Cao Y, Wang N, Lu Y *et al* 2020 *J. Sep. Sci.* **43** 954

Springer Nature or its licensor (e.g. a society or other partner) holds exclusive rights to this article under a publishing agreement with the author(s) or other rightsholder(s); author self-archiving of the accepted manuscript version of this article is solely governed by the terms of such publishing agreement and applicable law.